



# NILDE

Network Inter-Library Document Exchange

Il presente documento viene fornito attraverso il servizio NILDE dalla Biblioteca fornitrice, nel rispetto della vigente normativa sul Diritto d'Autore (Legge n.633 del 22/4/1941 e successive modifiche e integrazioni) e delle clausole contrattuali in essere con il titolare dei diritti di proprietà intellettuale.

**La Biblioteca fornitrice** garantisce di aver effettuato copia del presente documento assolvendo direttamente ogni e qualsiasi onere correlato alla realizzazione di detta copia.  
**La Biblioteca richiedente** garantisce che il documento richiesto è destinato ad un suo utente, che ne farà uso esclusivamente personale per scopi di studio o di ricerca, ed informare adeguatamente i propri utenti circa i limiti di utilizzazione dei documenti forniti mediante il servizio NILDE.

**La Biblioteca richiedente** è tenuta al rispetto della vigente normativa sul Diritto d'Autore e in particolare, ma non solo, a consegnare al richiedente un'unica copia cartacea del documento, distruggendo ogni eventuale copia digitale ricevuta.

**Biblioteca richiedente:** Facoltà di Medicina e Chirurgia- Università degli Studi dell'Aquila

**Data richiesta:** 25/10/2013 09:45:27

**Biblioteca fornitrice:** Biblioteca delle Scienze Mediche

**Data evasione:** 25/10/2013 10:05:32

**Titolo rivista/libro:** Neurosurgery

**Titolo articolo/sezione:** The clinical effects of deep brain stimulation of the pedunculopontine tegmental nucleus in movement disorders may not be related to the anatomical location

**Autore/i:** Mazzone P, Sposato S, Insola A, Scarnati E

**ISSN:** 0148-396X

**DOI:** 10.1227/NEU.0000000000000108

**Anno:** 2013

**Volume:** 73

**Fascicolo:** 5

**Editore:**

**Pag. iniziale:** 894

**Pag. finale:** 906

# The Clinical Effects of Deep Brain Stimulation of the Pedunculopontine Tegmental Nucleus in Movement Disorders May Not Be Related to the Anatomical Target, Leads Location, and Setup of Electrical Stimulation

Paolo Mazzone, MD\*  
 Stefano Sposato, MD‡  
 Angelo Insola, MD§  
 Eugenio Scarnati, PhD¶

\*Stereotactic and Functional Neurosurgery, CTO Hospital, ASL RMC, Rome, Italy; ‡Neuroradiology, CTO Hospital, ASL RMC, Rome, Italy; §Neurophysiopathology, CTO Hospital, ASL RMC, Rome, Italy; ¶Department of Applied Clinical and Biotechnological Sciences, University of L'Aquila, L'Aquila, Italy

**Correspondence:**  
 Paolo Mazzone, MD,  
 Operative Unit for Stereotactic and Functional Neurosurgery, ASL RMC, CTO Hospital, Via San Nemesio 21, 00145 Rome, Italy.  
 E-mail: stereomaz@libero.it

**Received,** February 9, 2013.  
**Accepted,** July 11, 2013.  
**Published Online,** July 17, 2013.

Copyright © 2013 by the  
 Congress of Neurological Surgeons

**BACKGROUND:** The pedunculopontine tegmental nucleus (PPTg) is a novel target for deep brain stimulation (DBS) in movement disorders.

**OBJECTIVE:** To clarify the relationships between the individual anatomic variations of the brainstem, the site in which the PPTg DBS is applied, and the clinical outcome in a relatively large number of patients affected by Parkinson disease or progressive supranuclear palsy.

**METHODS:** Magnetic resonance images have been used to evaluate brainstem anatomy and the relationships between lead position and specific brainstem landmarks. All data were matched on atlas representations of the PPTg and were correlated with Unified Parkinson Disease Rating Scale III (UPDRS III), subitems 27 to 30 of UPDRS III and the Hoehn and Yahr evaluations.

**RESULTS:** A high variance of brainstem parameters was evident, affecting the relationships between the position of the nucleus and lead contacts. According to the contacts giving the best clinical outcome, patients could be distinguished between those who required the use of 2 adjacent contacts and those who required stimulation through 2 nonadjacent contacts. Furthermore, in the former group the target coordinates were more lateral and deeper compared with the latter group.

**CONCLUSION:** Individual PPTg-DBS planning is required to overcome the inconsistencies linked to the high variability in the brainstem anatomy of patients. The lack of correlations between lead position, contact setup, and clinical outcome indicate that the benefits of PPTg DBS may not be strictly linked to the site of stimulation within the PPTg area, and may not depend upon the neurons still surviving in this region in Parkinson disease or progressive supranuclear palsy.

**KEY WORDS:** Brainstem anatomic landmarks, Deep brain stimulation, Electrical setup, Leads location, Neurological outcome, Pedunculopontine tegmental nucleus

Neurosurgery 73:894–906, 2013

DOI: 10.1227/NEU.0000000000000108

www.neurosurgery-online.com

The pedunculopontine tegmental nucleus (PPTg) is a pontomesencephalic structure involved in Parkinson disease (PD) and other neurodegenerative disorders.<sup>1–7</sup> Recently, it

has been introduced as a novel target for deep brain stimulation (DBS) in movement disorders.<sup>8,9</sup> The therapeutic benefits of PPTg DBS are not yet fully elucidated, although motor symptoms, in particular, the freezing of gait and axial disturbances, are positively affected.<sup>10–19</sup> The stereotactic implantation of electrodes for PPTg DBS has required the development of a new theoretical surgical approach far more complex than the standardized method conceived many years ago for traditional targets.<sup>20–25</sup> An early problem was the uncertainty about the location of the nucleus in the brainstem,

**ABBREVIATIONS:** DBS, deep brain stimulation; HY, Hoehn and Yahr; ML, medial lemniscus; PD, Parkinson disease; PH, Paxinos and Huang; PMJ, pontomesencephalic junction; PPTg, pedunculopontine tegmental nucleus; PSP, progressive supranuclear palsy; STN, subthalamic nucleus; UPDRS III, Unified Parkinson Disease Rating Scale III; VFL, ventricular floor line; FFL, fastigial floor line

unfamiliar to most neurosurgeons.<sup>26-28</sup> This difficulty was worsened by the fact that the available stereotactic atlases derived from a single brain, and traditional landmarks, such as the bicommissural line, may be inappropriate when applied to a nucleus embedded in a highly variable structure such as the human brainstem.<sup>29</sup> Moreover, when implanting electrodes for DBS, stochastic differences in the lead position commonly occur, which depend not only on anatomic individual differences from patient to patient, but also on surgical planning and/or adopted surgical techniques. Consequently, the site and volume of tissue affected by the configuration of the electrical field generated by the stimulation may vary.<sup>23,30</sup> Such factors, together with the heterogeneous selection of patients, stimulation of different subregions of the PPTg area, nonstandardized surgical planning, and different operative conditions that have characterized different studies, may have contributed to inconsistencies in previously reported clinical results. Given the relatively large number of patients who have undergone implantation in the PPTg from 2005 until the present in our hospital in this article, we attempted to evaluate the correlation between reference landmarks, variability of individual anatomy, coordinates of the targeted point, lead position inside the brainstem, and clinical results. This was done to answer 4 key questions: (1) To what extent was the individual variation of brainstem anatomy reflected in the position of the PPTg and stimulating lead? (2) Where were the leads with respect to the planned anatomic target? (3) Was the electrical configuration of active contact pairs related directly to the position of the lead or to the trajectory angles? (4) What, if any, was the relationship among landmarks, lead position, electrical configuration of contacts, and clinical results?

## SUBJECTS AND METHODS

### Subjects

The study was performed in 28 patients, 24 affected by PD and 4 by progressive supranuclear palsy (PSP). Their average age was  $61.2 \pm 13.9$  years (mean  $\pm$  SD; range, 43-76). All but 2 patients were male. Of the 28 patients, 2 were excluded from the correlation analysis, because 1 patient underwent microrecordings in an attempt to identify discharge patterns of PPTg neurons and was not implanted, and 1 patient experienced intraoperative bleeding in the right globus pallidus internus. The duration of disease before surgery was  $9.0 \pm 3.6$  years, and the postsurgical follow-up was  $3.8 \pm 1.5$  years. Details concerning the duration of disease, diagnosis, and typology of implantation are given in Table 1. Patients were recommended for surgery by neurologists on the basis of their main clinical symptoms. The surgical procedure was approved by the local ethics committee, and all patients provided a written personal informed consent.

### Methods

#### Preoperative Neuroradiology

T1 and T2 acquisitions of axial (volumetric), sagittal, and coronal magnetic resonance imaging (MRI) slices were performed (Philips, Gyroscan NT, 1.0 Tesla). The axial slices of the brainstem were taken parallel to the pontomesencephalic junction (PMJ) and perpendicular to the ventricular floor line (VFL). Slices were spaced at 0.5 mm, and the thickness of each axial slice was set at 1 mm to obtain MRI images that could reliably be compared with those reported in the Paxinos and Huang (PH) atlas (Figure 1A, B).

#### Anatomic Measurements

Anatomic measurements were made by using preoperative MRI according to the acquisition method described above. We adopted specific

**TABLE 1. Clinical Characteristics of Patients and Stimulation Parameters<sup>a</sup>**

Age	$61.2 \pm 13.9^b$	Range 43-76 y		
Sex	2 F (7.1%)	26 M (92.8%)		
Disease	4 PSP (14.2%)	24 PD (85.7%)		
Duration	$9.8 \pm 4.1^b$	Range 2-16 y		
Total operated patients	28			
Targeted PPTg	34 (1 patient microrecordings only)			
Implanted patients	27 (1 adverse event in right GPi)			
PPTg (n = 33)	Bilateral	6 (21.4%)	Unilateral	21 (78.5%) (1, left side)
Chronic DBS patients	26/28			
Follow-up	$3.8 \pm 1.5^b$ (1-6 years)			
DBS	Monopolar	0/26	Bipolar	26/26 patients
	Group 1 <sup>c</sup>	8/26 patients (30.7%)	Group 2 <sup>d</sup>	18/26 patients (69.2%)
Amplitude	$5.6 \pm 1.3^b$ V (PSP)		$3.3 \pm 1.0^b$ V (PD)	
Pulse width	60 $\mu$ s		60 $\mu$ s	
Rate	25 Hz (6 patients)		40 Hz (20 patients)	

<sup>a</sup>DBS, deep brain stimulation; PD, Parkinson disease; PPTg, pedunculopontine tegmental nucleus; PSP, progressive supranuclear palsy; GPi, globus pallidus internus.

<sup>b</sup>mean  $\pm$  SD.

<sup>c</sup>Tight configuration, requiring stimulation through 2 adjacent contacts.

<sup>d</sup>Spaced configuration, requiring stimulation through 2 not adjacent contacts.

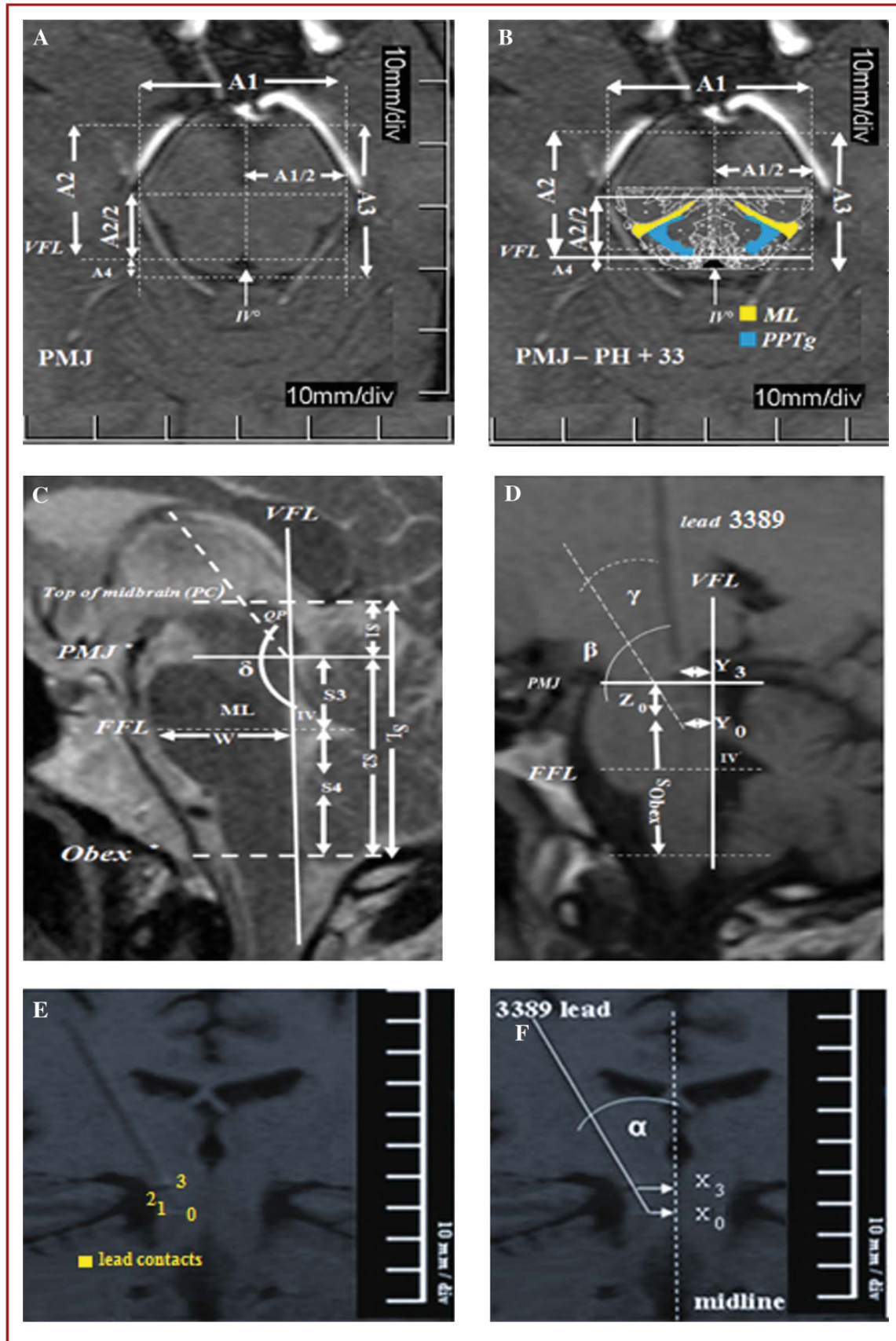


**FIGURE 1.** Anatomic and lead parameters. **A**, preoperative axial volumetric MRI taken at the level of the PMJ. **B**, the section +33 of the PH atlas is overlapped with the MRI section illustrated in **A**. The ML and the PPTg are highlighted in yellow and blue, respectively. **C**, sagittal anatomic landmarks represented on a preoperative MRI section. **D**, Y and Z lead parameters, and  $\beta$ - and  $\gamma$ -angles in a postoperative sagittal MRI section. **E**, coronal postoperative MRI section taken along the lead plane. **F**, the coronal  $\alpha$ -angle and the X parameter are reported in the same MRI section. FFL, fastigial floor line; ML, medial lemniscus; PH, Paxinos and Huang; PMJ, pontomesencephalic junction; PPTg, pedunculopontine tegmental nucleus; VFL, ventricular floor line.

brainstem measures to better detail the anatomy of the stereotactic space to target the PPTg (Figure 1).

The axial parameters were measured on axial volumetric MRI slices (Figure 1A, B) and designated with the letter A as follows: (1) The  $A_1$  distance, ie, the diameter of the pons between its lateral borders; (2) The  $A_{1/2}$  distance, corresponding to half of the distance of  $A_1$ , measured along the  $A_{2/2}$  line; (3) The  $A_2$  distance, between the anterior border of the pons and the VFL; (4) The  $A_{2/2}$  distance, ie, half of the  $A_2$  distance, drawn on a line tangent to the medial lemniscus (ML). This parameter corresponds to the distance between the VFL and a line tangent to the ML representation, running parallel to the VFL itself. In our practice this is the most useful parameter to establish on MRI the Y coordinate (Figure 1A, B); (5) The  $A_3$  distance, ie, the diameter of the pons between its anterior and posterior borders measured along the midline; and (6) The  $A_4$  distance, between the VFL and the posterior border of the pons. We also considered the variables  $\Delta A_{1/2}$  ( $A_{1/2}$ MRI- $A_{1/2}$ PH) and the  $\Delta A_{2/2}$  ( $A_{2/2}$ MRI- $A_{2/2}$ PH), which were the differences between the  $A_{1/2}$  and the  $A_{2/2}$  distance resulting from the comparison of MRI-based and PH atlas-based individual measurements.

The sagittal parameters were measured on sagittal MRI slices (Figure 1C) and designated with the letter S as follows: (1) The  $S_1$  distance, from the plane formed by the top of the midbrain, considered at the middle point of the posterior commissure, to the PMJ; (2) The  $S_2$  distance, between the PMJ and the Obex; (3) The  $S_L$  distance, between the top of the midbrain and the Obex, representing the length of the brainstem (long axis); (4) The  $S_W$  distance, corresponding to the width of the pons measured along the fastigial floor line (FFL). This line starts from the fastigial point (F) and runs parallel to the PMJ; (5) The  $S_3$  distance, between the PMJ and the FFL; (6) The  $S_4$  distance, between the Obex and the FFL; and (7) The  $\delta$  angle, formed by the VFL and the quadrigeminal plate. This angle provides an index of the vertical extension of the midbrain, because the further it approaches 180°, the greater the height of the midbrain (Figure 1C).

### Surgical Procedure

We used the same procedure described in detail in previous studies.<sup>22,23,30</sup> All patients were implanted with the quadripolar 3389 DBS lead (Medtronic, Minneapolis, Minnesota, Neurological Division). In brief, the plan to target the PPTg was based on stereotactic angio-computed tomography (CT) scans by using the PMJ as a major reference point and also taking into account the VFL and the Obex. The 3-D reconstruction of the cerebral vascular system, made by means of the navigation Maranello Stereotactic System (CLS Titanium, Forlì, Italy), allowed us to exclude the possibility that any conflict could occur between the chosen lead trajectory and the vessels.

### Postoperative Neuroradiology

The correct positioning of the lead was also confirmed in 24 patients by postsurgical MRI, and in 3 patients by CT, because the latter patients had claustrophobia that made MRI impossible. Postoperative MRI,

acquired by using the same method of preoperative imaging, allowed us to evaluate the spatial relationships between the lead contacts and anatomic brainstem landmarks, such as the PMJ, VFL, and FFL, and to calculate the coordinates Y (millimeters in front of the VFL),  $Z_o$  (millimeters below the PMJ) (Figure 1D), X (millimeters from the pontine midline) (Figure 1E, F), and the inclination of the lead trajectory (coronal  $\alpha$ -angle, sagittal  $\beta$ -angle, sagittal  $\gamma$ -angle between the lead trajectory and the tangent to the medial lemniscus) (Figure 1D, F). The distance of contact 0 from the Obex ( $S_{Obex}$ ) was taken into account when evaluating the difference from patient to patient in the lead depth in the pons.<sup>21</sup> To appropriately overlap data from MRI on the PH atlas, we identified the axial slice in the PH atlas in which the PMJ may be recognized, ie, the +33 slice (Figure 1A, B), such that this slice served as a reliable reference for reconstructing the brainstem.

### Atlas-based 3-D Reconstruction of PPTg Anatomy

A 3-D representation of the PPTg was obtained by combining the PH atlas slices +31, +33, and +35 (Figure 2A, B). Because the 2-D slices are not reported at the same magnification in the PH atlas, it was necessary to normalize them before applying for the reconstruction of the measurements performed on the preoperative MRI of each patient to calculate the variability of anatomic distances ( $\Delta A_{1/2}$  and  $\Delta A_{2/2}$ ) (Figure 3B, C; Figure 4A, B and Figure 5). The Rhinoceros software ver.3 SR4 was used for constructing the 3-D representations from 26 patients, and data were included in the Medico-Cad planning navigational tool of the Maranello Stereotactic System (CLS-Titanium, Forlì, Italy). The same method was adopted in the 3-D representation of the 3389 lead and the active contacts in real size (Figure 2A, B).

### Stimulation and Clinical Postoperative Follow-up

The electrode implantation was followed over a 15-day test period in which patients were studied in order to verify if any effect due to the mere mechanical presence of the lead occurred. Once this possibility was excluded, clinical evaluation was performed in both OFF DBS and ON DBS conditions, before the definitive application of the pulse generator (Kinetra or Solettra, Medtronic, Minneapolis, Minnesota, Neurological Division). Thereafter, the stimulation was tested varying the electrical configurations, ie, monopolar vs bipolar, high frequency vs low frequency, continuous vs cyclic. The neurological examination was done by evaluating the Unified Parkinson Disease Rating Scale III (UPDRS III) and subitems 27 to 30<sup>31</sup> in different conditions, ie, OFF drugs/OFF DBS, ON drugs/OFF DBS, OFF drugs/ON DBS, and finally, ON drugs/ON DBS. The Hoehn and Yahr (HY) disability scale was used (Table 2) to assess the reduction in the severity of clinical aspects of the disease.<sup>32,33</sup> Clinical examinations were repeated every 3 months. If required, resetting of stimulation was performed. The clinical results following 1 month of continuous DBS are reported in Table 2. Having, to date, all 28 patients completed the first year of follow-up, we included in the study only data concerning this period of time.

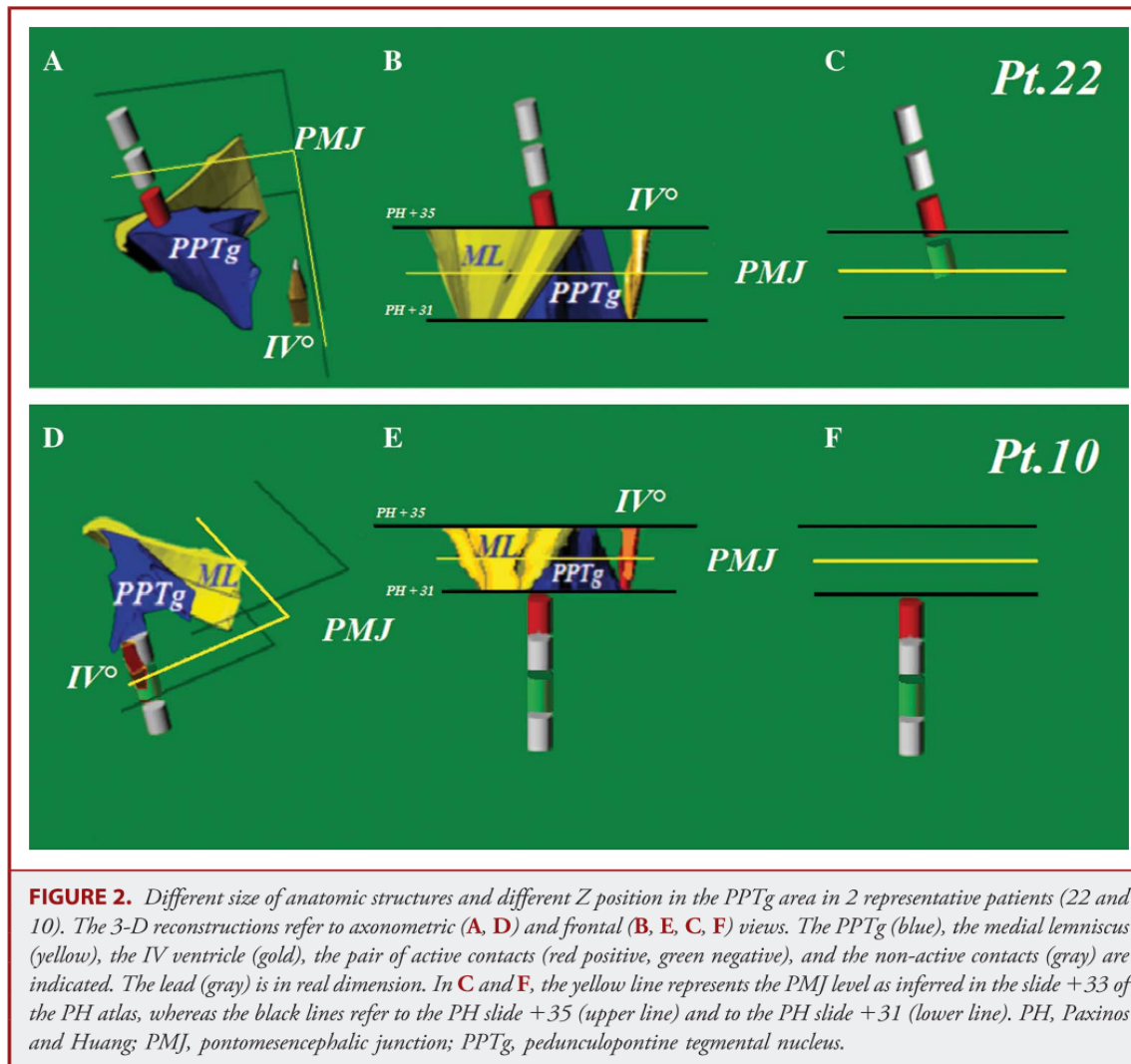


**FIGURE 2.** Different size of anatomic structures and different Z position in the PPTg area in 2 representative patients (22 and 10). The 3-D reconstructions refer to axonometric (A, D) and frontal (B, E, C, F) views. The PPTg (blue), the medial lemniscus (yellow), the IV ventricle (gold), the pair of active contacts (red positive, green negative), and the non-active contacts (gray) are indicated. The lead (gray) is in real dimension. In C and F, the yellow line represents the PMJ level as inferred in the slide +33 of the PH atlas, whereas the black lines refer to the PH slide +35 (upper line) and to the PH slide +31 (lower line). PH, Paxinos and Huang; PMJ, pontomesencephalic junction; PPTg, pedunculopontine tegmental nucleus.

**Statistical Analysis**

Anatomic aspects and clinical outcomes were evaluated in relation to lead configuration using one-way analysis of variance with stimulation setup (pair of active contacts and polarity) as the independent variable. Pairwise comparisons of motor and functional scores of the baseline and follow-up evaluations were made with the nonparametric Mann-Whitney *U* matched-pairs test. Correlation between anatomic parameters, clinical outcomes, stimulation setup, and lead position was assessed by calculating the Spearman  $\rho$  and the percentage of correlation (*P* value). Statistical analyses were conducted using the SPSS v. 9.0 statistical package with significance set at *P* = .05. All data were presented as mean  $\pm$  SD.

**RESULTS**

**Surgery**

No adverse events occurred during or after PPTg surgery. Two patients died 7 years after the surgical procedure of supervening diseases, unrelated to PPTg implantation and to their neurological disease. Unfortunately, it was not possible to conduct autopsy verification of their brains. Oscillopsia, trigeminal pain, and urinary incontinence were not observed during either the post-

surgical follow-up or PPTg stimulation. The most common consequences of PPTg DBS were paresthesias in the hemisomi contralateral to the implanted side which were felt by patients as PPTg DBS was initiated or in coincidence with modifications of electrical parameters, in particular, when stimulation amplitude was increased (Table 1). Over time, perception of paresthesias decreased and finally disappeared.

**DBS Configuration and Patient Groups**

The clinical characteristics of patients and stimulation parameters are summarized in Table 1. All patients were stimulated with electrodes in a bipolar configuration. Of the 26 patients implanted for chronic DBS, 14 were stimulated with the contact 1(-) and contact 3(+) pair. The 0(-) contact was used in combination with the contact 1(+) in 5 patients, and with contact 3(+) in 4 patients. Three patients required stimulation through the intermediate pair configured as 1(-) and 2(+) (Figure 4A). Thus, it was evident that, as far as contact configuration was concerned, patients could be distinguished between those who required activation of a pair of adjacent

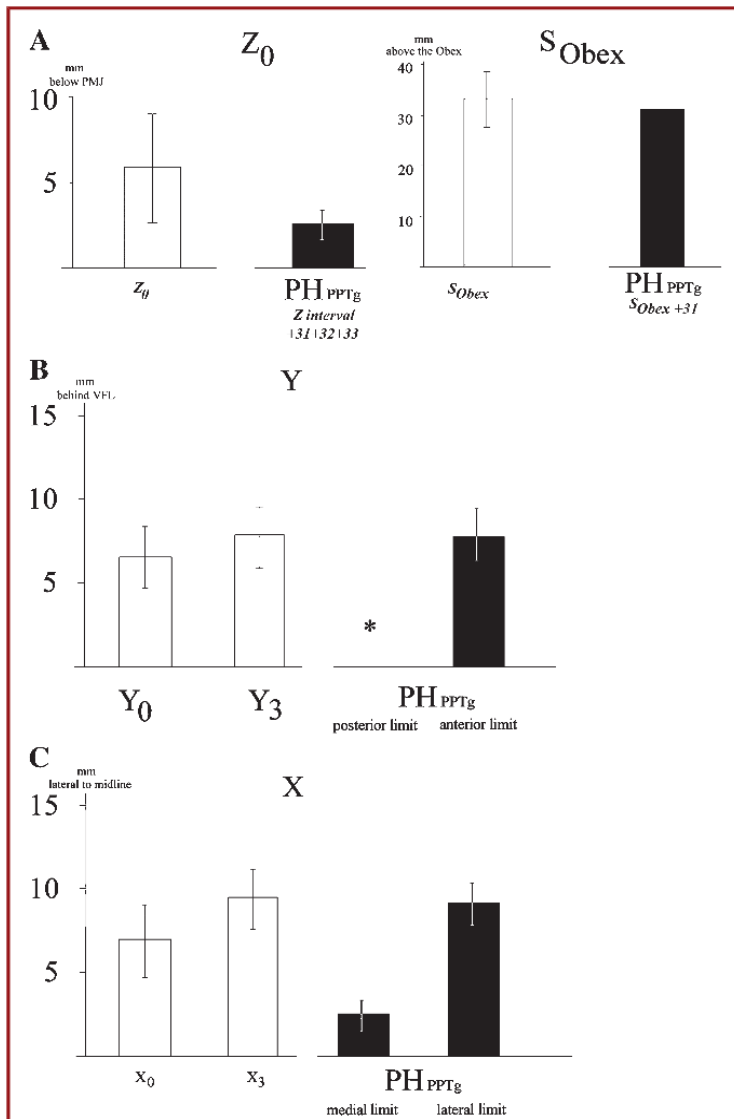


**FIGURE 3.** Patients coordinates and atlas PPTg representation. **A**, bar graph comparing the patients (white bars) mean values  $\pm$  SD of the  $Z_0$  and  $S_{Obex}$  coordinates with respect to the position of the PPTg as represented in the PH atlas (black bars). **B**, comparison of patients  $Y_0$  and  $Y_3$  coordinates and the anteroposterior limits of the PPTg in the PH atlas. The asterisk indicates the location of the VFL that has been considered as the zero point for the calculation of coordinates. **C**, comparison of patients  $X_0$  and  $X_3$  coordinates and the laterolateral limits of the PPTg, as represented in the PH atlas. PH, Paxinos and Huang; PMJ, ponto mesencephalic junction; PPTg, pedunculopontine tegmental nucleus; VFL, ventricular floor line.

contacts (tight configuration; group 1, 8 patients), and those who required activation of a pair of contacts spaced by at least 1 contact (broad configuration; group 2, 18 patients) (Figure 6E). Contrary to the 25-Hz frequency of stimulation applied in the first 6 patients, a stimulation frequency of 40 Hz was delivered in all the other patients. Patients affected by PSP required higher-voltage stimuli ( $5.6 \pm 1.3$  V) than those required by PD subjects ( $3.3 \pm 1.2$  V). In all patients, the pulse width was 60  $\mu$ s (Table 1).

### Comparison of Anatomic Landmarks Between Atlas-based and Patient-based Measurements

The value of the variable  $\Delta A_{1/2}$  based on the patients' anatomy did not significantly differ from the reference value calculated in the PH atlas. However, in the PH atlas, no measurement could be made concerning the  $A_2$  and  $A_3$  distances, because the atlas does not include the anterior part of the brainstem where these parameters may be measured. The  $A_{2/2}$  value varied in the PH atlas slices, and therefore the average value of 14.5, resulting from the measurements of slides +31, +33, and +35, was taken as the atlas reference and used to calculate the variable  $\Delta A_{2/2}$  in the patient's brainstem. From the analysis of data, it is evident that the largest variance was in the  $A_1$  distance; thus, among the axial parameters of the human brainstem the laterolateral extension had the greatest variability between patients.

In comparing the values of sagittal parameters between group 1 and group 2, a statistically significant difference occurred only for the distance  $S_W$  ( $P = .05$ ).

### Correspondences of the PMJ Level Between PH Atlas and MRI Slice

In the slice +33 of the PH atlas, the inferior colliculus has the largest representation; the dorsocaudal representation of IV ventricle begins to appear and the nucleus of the IV cranial nerve is present; thus, this slice may be considered as a slice taken at the PMJ level. The slices +34, +35, and +36, which include the representation of the aqueduct, may be considered as located above the PMJ, whereas the slices +32 and +31 may be considered as located below the PMJ, the latter slice representing the inferior border of the PPTg.

### UPDRS III, Subitems 27 to 30, and HY Evaluations

The UPDRS III score in the OFF drugs/OFF DBS condition was  $70.2 \pm 16.5$  at 1 month of follow-up. In the ON drugs/OFF DBS condition, the score was  $34.9 \pm 12.8$ , significantly lower in comparison with the previous condition ( $P = .001$ ). A significant reduction in the UPDRS III was also obtained in the OFF drugs/ON DBS condition ( $28.9 \pm 11.3$ ,  $P = .001$ ). An improvement in UPDRS, although not significant ( $P = .07$ ), was observed during the OFF drugs/ON DBS treatment compared with the ON drugs/OFF DBS condition (Table 2). A significant improvement in the UPDRS score was also obtained by combining drug therapy and DBS ( $23.5 \pm 2.3$ ) in comparison with the OFF drugs/OFF DBS condition ( $P = .001$ ). The differences between drug or DBS therapy alone and combined treatment did not reach the level of statistical significance ( $P = .1$  for both comparisons).

The score of subitems 27 to 30 in the OFF drugs condition was  $5.2 \pm 2.2$ , whereas in the ON DBS condition (CAPIT), it improved to  $2.9 \pm 1.0$  ( $P = .001$ ). The difference between preoperative and postoperative HY scores was also significant ( $3.7 \pm 0.6$  and  $2.2 \pm 0.8$ , respectively,  $P = .001$ ) (Table 2).

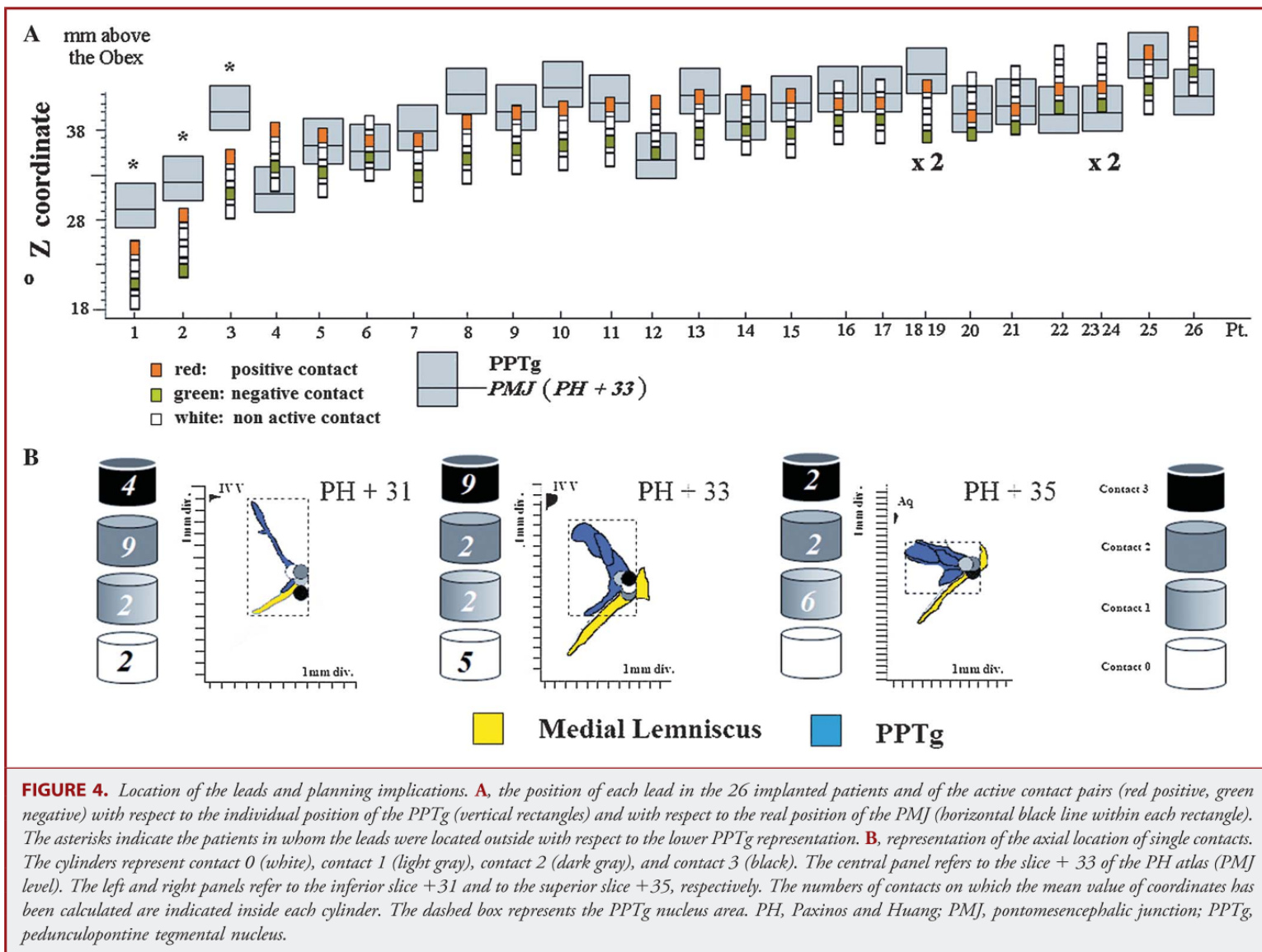


**FIGURE 4.** Location of the leads and planning implications. **A**, the position of each lead in the 26 implanted patients and of the active contact pairs (red positive, green negative) with respect to the individual position of the PPTg (vertical rectangles) and with respect to the real position of the PMJ (horizontal black line within each rectangle). The asterisks indicate the patients in whom the leads were located outside with respect to the lower PPTg representation. **B**, representation of the axial location of single contacts. The cylinders represent contact 0 (white), contact 1 (light gray), contact 2 (dark gray), and contact 3 (black). The central panel refers to the slice + 33 of the PH atlas (PMJ level). The left and right panels refer to the inferior slice +31 and to the superior slice +35, respectively. The numbers of contacts on which the mean value of coordinates has been calculated are indicated inside each cylinder. The dashed box represents the PPTg nucleus area. PH, Paxinos and Huang; PMJ, pontomesencephalic junction; PPTg, pedunculopontine tegmental nucleus.

The percent change ( $\Delta$  %) of both the UPDRS III and HY scale was significantly correlated with the values of contacts  $X_0$  and  $X_3$  and of the  $S_{Obex}$  (Table 2).

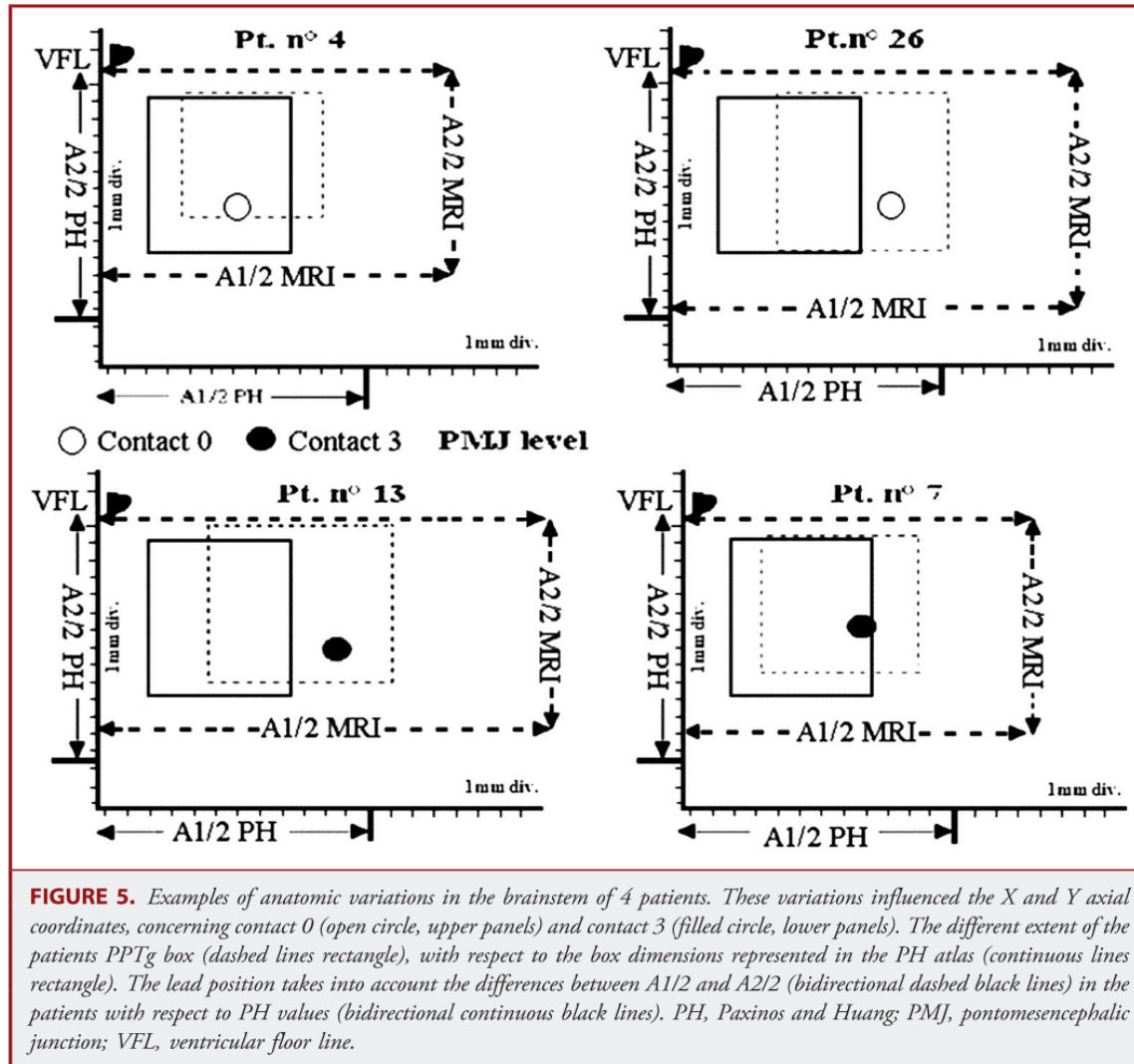
**Positions of the Leads and Angles of Trajectories: Correlation Between Anatomic Data, Lead Location, Clinical Outcomes, and Electrical Setup**

The lead was oriented at  $83.3 \pm 7.3^\circ$  in the anteroposterior direction with respect to the PMJ, according to the  $S_B$  angle (Figure 1D). In 10 of 27 patients, the inclination was exactly  $90^\circ$  with respect to the PMJ. Thus, in these 10 patients, the 4 contacts shared exactly the same distance from the VLF. The  $S_\gamma$ -angle had a value of  $21.2 \pm 6.2^\circ$ . No statistically significant difference was observed when comparing the variance of the  $S_B$ -angle ( $53.3^\circ$ ) and the variance of the  $\delta$ -angle ( $54.7^\circ$ ). The inclination of the lead trajectory in the coronal plane, expressed by the  $C\alpha$ -angle, was  $17.3 \pm 5.0^\circ$  (Figure 1F).

The values of X, Y, and  $Z_0$  coordinates, and the measure of  $S_{Obex}$  were evaluated and compared with the PH representation (Figures 1D, F and 3 A-C). The  $Z_0$  and  $S_{Obex}$  parameters, which give the depth of the lead with respect to the PMJ and the Obex, respectively, were influenced both by the height of the pons and by the anatomic individual variability of the position of the PMJ. If we consider each single lead position and the configuration of active contacts compared with the individual PMJ position and the craniocaudal PPTg representation, we may conclude that 3 patients had the lead contacts outside the lower atlas-based representation of the nucleus (Figure 4A). The lead position was not significantly correlated with the anatomic data ( $P = .05$ , analysis of variance), nor did statistical analysis demonstrate any correlation between the X, Y, and Z coordinates and the  $A_2$ ,  $A_{1/2}$ , and  $A_{2/2}$  values, respectively.

Also, there was no correlation between improvements in UPDRS III and HY score and the variables  $\Delta A_{1/2}$  and  $\Delta A_{2/2}$ , and thus the anatomic variability of the patients brainstem with respect to the atlas-based values did not influence either the





contacts configuration or the clinical outcome. When comparing the anatomic variables between group 1 and group 2 patients, no statistically significant difference was observed (Table 3).

The X and Y coordinates for each single contact, in relation to the axial plane of the PPTg crossed by the lead, are reported in Table 4. These values were represented on the corresponding level in the PH axial slices where contacts appeared to be placed in a correct position with respect to the boundaries of the nucleus (Figure 4B). The representation of the mean values of contact location on the PH slices did not require any graphic manipulation, and values were reported as they were in graphical form (Figure 4B). It should be emphasized that, in planning the surgery, the anatomic differences from patient to patient were taken into account with respect to the dimension of structures reported in the PH atlas, in particular, for establishing the X and Y coordinates, as illustrated in Figure 5.

#### Contacts Configurations and Leads Location: Clinical Impact

There was no difference in the clinical outcome in patients in both groups 1 and 2; accordingly, no statistically significant

difference was noted in basal condition in the total score of UPDRS III ( $P = .13$ ), in the HY scale ( $P = .34$ ) and in subitems 27 to 30 of the UPDRS ( $P = .85$ ). Both groups significantly improved ( $P = .001$ ) in UPDRS III, in 27 to 30 subitems and in HY disability score during the postsurgical follow-up, ie, irrespective of the configuration of the pair of active contacts (Figure 6 A-C, upper panels). Conversely, group 1 patients showed a significant improvement in comparison with group 2 patients when they were evaluated according to the percentage of improvement in HY scale (Figure 6A, lower panel). According to the measurements made on postsurgical MRI slices, in group 1 patients the lead was located more distal to the midline (X coordinate) ( $P = .05$ ) and deeper ( $S_{\text{Obex}}$  distance) ( $P = .03$ ) in comparison with group 2 patients (Figure 6D).

#### DISCUSSION

The present study was based on the analysis of anatomic data concerning the pontomesencephalic region in 28 patients affected by PD or PSP, who underwent PPTg DBS to control gait and axial disturbances. Measurements of landmarks done on MRI slices

**TABLE 2. Clinical Evaluation (1 Month of Continuous PPTg DBS)<sup>a</sup>**

Drugs	PPTg	UPDRS III	Subitems 2730	HY
OFF	OFF	70.2 ± 16.5*	5.2 ± 2.2 <sup>o</sup>	3.7 ± 0.6*
ON	OFF	34.9 ± 12.8 <sup>◇</sup>	4.1 ± 1.2	3.1 ± 0.4
OFF	ON	28.9 ± 11.3 <sup>□</sup>	2.9 ± 1.0 <sup>oo</sup>	2.2 ± 0.8**
ON	ON	23.5 ± 11.1 <sup>◆</sup>	2.5 ± 0.4	2.0 ± 0.2
		<b>Δ UPDRS III</b>	<b>Δ Subitems</b>	<b>Δ HY</b>
		59.2 ± 10.5	40.7 ± 10.5	38.5 ± 18.8

**Anatomoclinical Correlation Analysis**

Δ UPDRS III			Δ HY		
Variables	Spearman ρ	P Value	Variables	Spearman ρ	P Value
X <sub>0</sub>	.5	.003	X <sub>0</sub>	.5	.009
X <sub>3</sub>	.04	.042	X <sub>3</sub>	.5	.004
S <sub>Obex</sub>	.4	.039	S <sub>Obex</sub>	.4	.023

<sup>a</sup>ANOVA, analysis of variance; DBS, deep brain stimulation; HY, Hoehn and Yahr; PPTg, pedunculopontine tegmental nucleus; UPDRS III, Unified Parkinson Disease Rating Scale III.  
<sup>◇</sup>◆ P= .001 vs\*, ANOVA.  
<sup>oo</sup> P= .001 vs <sup>o</sup>, ANOVA.  
<sup>••</sup> P= .001 vs \*, ANOVA.

$$\text{Formula for } \Delta\text{UPDRS III} = \frac{\text{OFF drugs/OFF DBS} - \text{OFF drugs/ON DBS}}{\text{OFF drugs/OFF DBS}}$$

$$\text{Formula for } \Delta\text{subitems} = \frac{\text{OFF drugs} - \text{ON DBS}}{\text{OFF drugs}}$$

$$\text{Formula for } \Delta\text{HY} = \frac{\text{OFF drugs} - \text{ON DBS}}{\text{OFF drugs}}$$

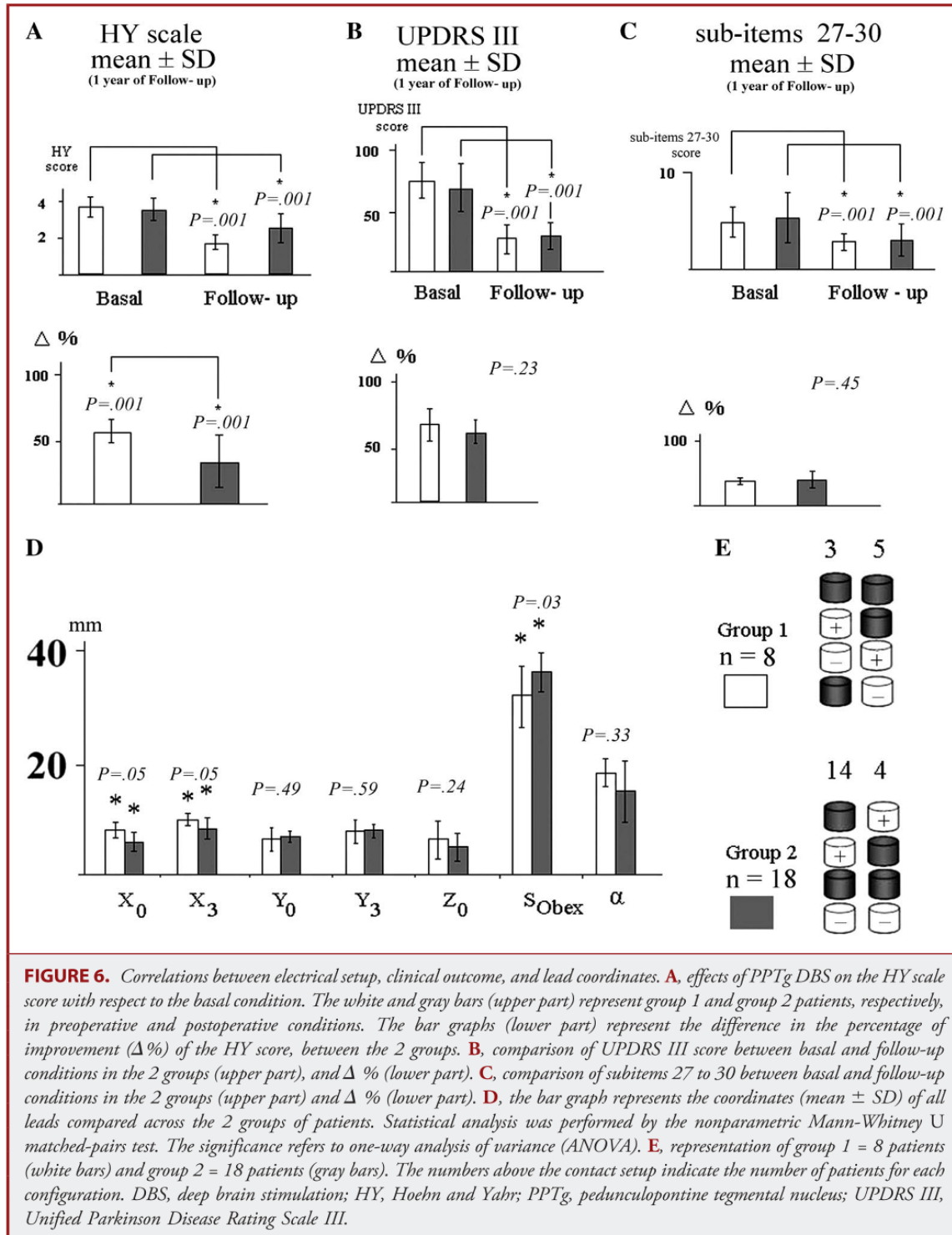
showed considerable individual variability from patient to patient, which was appropriately considered during the surgical planning to target the PPTg. This variability is critical in establishing the spatial representation of the PPTg and makes the identification and representation of the PPTg obtained from the Schaltenbrand and Wharen atlas, which is based on the anatomy of a single brain, unreliable. In our opinion, when dealing with brainstem neurosurgery, the marked variability of the height of the mesencephalon with respect to the PMJ is a major factor that makes the use of traditional landmarks such as the bicommissural line and the posterior commissure for determining stereotactic coordinates useless.<sup>22,23,30</sup>

Despite the fact that the Schaltenbrand and Wharen atlas<sup>34</sup> is the only neurosurgical atlas illustrating the brainstem (albeit in part), we preferred the PH brainstem atlas<sup>35</sup> to represent and illustrate our pre- and postsurgical data. This choice was motivated by the detailed description of brainstem structure in PH atlas slices.<sup>35</sup> A crucial aspect of our method was the identification of the PMJ level on the +33 slice of the PH atlas.<sup>35</sup> This slice represented a reliable reference to exactly translate measurements done on MRI in graphical form, thus allowing us to evaluate correlation between anatomic, electrical, and clinical data. This reconstruction, which required the use of complex

informatics and mathematical procedures, provided the basis first for a 2-D and then a 3-D representation of brainstem structures. The 3-D spatial representations also provided a valuable tool to understand where stimulation was applied in the brainstem and to investigate whether any correlation occurred between anatomic data and clinical outcome.

The lack of a statistically significant correlation between the landmarks used for the surgical planning could be explained by the fact that the planning was based on the individual anatomic parameters of each patient rather than on absolute values.

The statistical analysis revealed that the electrical setup was not correlated with the clinical scores. However, in some patients, the best clinical outcome was obtained with the lead positioned in a more lateral and deeper position than in other patients and with 2 adjacent contacts as the active pair for stimulation delivery. This finding suggests the existence within the PPTg area of a region whose stimulation may give a better clinical result. Surprisingly, however, a good clinical effect was also observed when stimulation was applied in a site close to the spatial representation of the PPTg (Figure 2A, B). Thus, there could be no specific area within or adjacent to the PPTg in which stimulation consistently provides the best clinical result. Assuming that stochastic variations of lead position could have occurred,<sup>21</sup> these would not have influenced



the clinical results, as also commonly conceived for DBS of the subthalamic nucleus (STN). These observations raise the possibility that the effectiveness of the PPTg DBS might not be mediated by an action directly exerted on those neurons not yet degenerated in the PPTg in PD and PSP.<sup>1-4,6,36,37</sup>

The pontotegmental region located posterior to the ML includes the PPTg and is known to be primarily involved in the control of gait and posture.<sup>2,38</sup> However, there is no proof

of a somatotopic organization of this region in the human brain; thus, the results of the PPTg DBS can not be site-specific when the stimulation is applied within this region in which, in addition to poorly defined neuronal populations, descending axonal bundles also run.<sup>39</sup> In such circumstances, the PPTg would be considered as a functional point within a region that is strategic for DBS application in movement disorders.

**TABLE 3. Correlation Analysis Between Anatomic Parameters, Pathology and Lead Configuration**

Anatomic Parameters			Pathology			
Variables	A2 Spearman ρ	P Value	Variables	PD (22/26) Mean ± SD (Range)	PSP (4/26) Mean ± SD (Range)	P Value
S <sub>w</sub>	.042	.021	X <sub>0</sub>	6.9 ± 1.4 (5-10)	4.2 ± 2.8 (0-6)	.007
S <sub>3</sub>	-.621	.001	X <sub>3</sub>	8.9 ± 1.1 (7-11)	7.0 ± 3.3 (2-9)	.035
S <sub>4</sub>	.552	.005	α	6.5 ± 3.7 (12-23)	22.0 ± 8.6 (12-30)	.043

Anatomic Parameters			Lead setup			
Variables	Δ A2/2 Spearman ρ	P Value	Variables	Group 1 (8/26) Mean ± SD (range)	Group 2 (18/26) Mean ± SD (range)	P Value
S <sub>w</sub>	.455	.020	X <sub>0</sub>	7.8 ± 1.4 (6-10)	5.8 ± 1.7 (0-8)	.011
S <sub>3</sub>	-.611	.001	X <sub>3</sub>	0.7 ± 0.8 (9-11)	8.1 ± 1.8 (2-11)	.010
S <sub>4</sub>	.533	.003	S <sub>obex</sub>	36.4 ± 3.3 (30-40)	31.8 ± 5.4 (18-41)	.039

Given that the Medtronic 3389 electrode we used spans a distance of 8 mm from the deepest to most superficial contact and that the length of the PPTg is approximately 1 cm, we can not exclude the possibility that stimulation involved structures close to the PPTg, such as the cuneiform nucleus,<sup>40</sup> at least in those patients in whom the deepest contact was located at the level of the PMJ. Thus, according to our results, we have to assume that there may be substantial differences between STN DBS and PPTg DBS. Although the effects of STN DBS may depend on the STN neuronal population spared in PD, the effects of PPTg DBS may not be strictly linked to neurons still surviving in the PPTg region in both PD and PSP. Activation of fibers passing close or within the stimulated region may contribute to the positive effects of PPTg DBS on those symptoms that are not influenced by dopaminergic mechanisms or responsive to STN DBS, such as postural instability and gait disorders.<sup>14-19,30,36,41</sup> In this regard, it is also worth noting that the chronaxie of fibers is lower than that of cells, so that stimuli in the 50- to 100-μs range preferentially activate fibers.<sup>24,42</sup>

**TABLE 4. X and Y Axial Coordinates (Mean ± SD) of Lead Contacts Crossing the PH Atlas Slices<sup>a</sup>**

	Lead 3389	Contact 0	Contact 1	Contact 2	Contact 3
Slice					
X					
	+ 31	6.5 ± 0.7	7.7 ± 0.3	7.7 ± 1.1	6.0 ± 1.4
	+ 33 (PMJ)	7.8 ± 1.8	7.5 ± 0.7	8.2 ± 0.3	8.6 ± 2.8
	+ 35	—	8.2 ± 1.4	8.2 ± 0.3	9.0 ± 0.0
Y					
	+ 31	6.0 ± 1.4	7.2 ± 0.3	6.5 ± 2.1	8.0 ± 1.1
	+ 33 (PMJ)	6.8 ± 0.4	6.5 ± 1.0	7.5 ± 0.7	7.0 ± 2.2
	+ 35	—	7.2 ± 0.4	7.2 ± 1.0	8.0 ± 1.4

<sup>a</sup>PH, Paxinos and Huang; PMJ, pontomesencephalic junction.

The clinical outcome in our patients deserves particular attention in comparison with the small cohorts of patients reported in the literature<sup>9,10,14,16,17</sup> and with the large body of clinical results arising from DBS of the STN.<sup>43,44</sup> The different results for PPTg DBS reported by other authors<sup>9,10,14,16,17</sup> may be due to several factors. In general, patients in our selection were younger than those implanted by other authors; thus, neuronal degeneration could have affected patients at different degrees. Furthermore, the several implantations we have performed allowed us to refine and standardize the targeting and the stimulation procedures as the number of patients increased, and the final position of an active contacts pair could have played a crucial role in determining differences in the clinical outcome.<sup>13,21,25,36,45,46</sup>

**CONCLUSION**

The innovative methodology and data reported in the present article offer the basis for a rational neurosurgical approach to PPTg, and help us to understand the relationships between the lead position, as commonly verified by MRI, and the anatomy of the brainstem reported in human atlases. Moreover, the data provide new aspects that may contribute to explaining the functioning of DBS in the pons.

**Disclosures**

The authors have no personal, financial, or institutional interest in any of the drugs, materials, or devices described in this article. Dr Scarnati was supported by a 2008 COFIN grant.

**REFERENCES**

1. Braak H, Del Tredici K. Cortico-basal ganglia-cortical circuitry in Parkinson's disease reconsidered. *Exp Neurol*. 2008;212(1):226-229.
2. Garcia-Rill E. The pedunculopontine nucleus. *Prog Neurobiol*. 1991;36(5):363-389.
3. Jellinger KA. The pedunculopontine nucleus in Parkinson's disease, progressive supranuclear palsy and Alzheimer's disease. *J Neurol Neurosurg Psychiatry*. 1988;51(4):540-543.

4. Jenkinson N, Nandi D, Muthusamy K, et al. Anatomy, physiology, and pathophysiology of the pedunculopontine nucleus. *Mov Disord.* 2009;24(3):319-328.
5. Lee MS, Rinne JO, Marsden CD. The pedunculopontine nucleus: its role in the genesis of movement disorders. *Yonsei Med J.* 2000;41(2):167-184.
6. Manaye KF, Zweig R, Wu D, et al. Quantification of cholinergic and select non-cholinergic mesopontine neuronal populations in the human brain. *Neuroscience.* 1999;89(3):759-770.
7. Pahapill PA, Lozano AM. The pedunculopontine nucleus and Parkinson's disease. *Brain.* 2000;123(pt 9):1767-1783.
8. Mazzone P, Lozano A, Stanzione P, et al. Implantation of human pedunculopontine nucleus: a safe and clinically relevant target in Parkinson's disease. *Neuroreport.* 2005;16(17):1877-1881.
9. Plaha P, Gill SS. Bilateral deep brain stimulation of the pedunculopontine nucleus for Parkinson's disease. *Neuroreport.* 2005;16(17):1883-1887.
10. Ferraye MU, Debu B, Fraix V, et al. Effects of pedunculopontine nucleus area stimulation on gait disorders in Parkinson's disease. *Brain.* 2010;133(pt 1):205-214.
11. Follett KA, Torres-Russotto D. Deep brain stimulation of globus pallidus interna, subthalamic nucleus, and pedunculopontine nucleus for Parkinson's disease: which target? *Parkinsonism Relat Disord.* 2012;18(suppl 1):S165-S167.
12. Hazrati LN, Wong JC, Hamani C, et al. Clinicopathological study in progressive supranuclear palsy with pedunculopontine stimulation. *Mov Disord.* 2012;27(10):1304-1307.
13. Mazzone P, Padua L, Falisi G, Insola A, Florio TM, Scarnati E. Unilateral deep brain stimulation of the pedunculopontine tegmental nucleus improves oromotor movements in Parkinson's disease. *Brain Stimul.* 2012;5(4):634-641.
14. Moro E, Hamani C, Poon YY, et al. Unilateral pedunculopontine stimulation improves falls in Parkinson's disease. *Brain.* 2010;133(pt 1):215-224.
15. Ostrem JL, Christine CW, Glass GA, Schrock LE, Starr PA. Pedunculopontine nucleus deep brain stimulation in a patient with primary progressive freezing gait disorder. *Stereotact Funct Neurosurg.* 2010;88(1):51-55.
16. Peppe A, Pierantozzi M, Chiavalon C, et al. Deep brain stimulation of the pedunculopontine tegmentum and subthalamic nucleus: effects on gait in Parkinson's disease. *Gait Posture.* 2010;32(4):512-518.
17. Thevathasan W, Coyne TJ, Hyam JA, et al. Pedunculopontine nucleus stimulation improves gait freezing in Parkinson disease. *Neurosurgery.* 2011;69(6):1248-1253.
18. Thevathasan W, Pogosyan A, Hyam JA, et al. A block to pre-prepared movement in gait freezing, relieved by pedunculopontine nucleus stimulation. *Brain* 2011; 134(pt 7):2085-2095.
19. Wilcox RA, Cole MH, Wong D, Coyne T, Silburn P, Kerr G. Pedunculopontine nucleus deep brain stimulation produces sustained improvement in primary progressive freezing of gait. *J Neurol Neurosurg Psychiatry.* 2011;82(11):1256-1259.
20. Benabid AL, Torres N. New targets for DBS. *Parkinsonism Relat Disord.* 2012;18(suppl 1):S21-S23.
21. Insola A, Valeriani M, Mazzone P. Targeting the pedunculopontine nucleus: a new neurophysiological method based on somatosensory evoked potentials to calculate the distance of the deep brain stimulation lead from the Obex. *Neurosurgery.* 2012; 71(1 suppl operative):96-103.
22. Mazzone P, Sposato S, Insola A, Dilazzaro V, Scarnati E. Stereotactic surgery of nucleus tegmenti pedunculopontine. *Br J Neurosurg.* 2008;22(suppl 1):S33-S40.
23. Mazzone P, Insola A, Sposato S, Scarnati E. The deep brain stimulation of the pedunculopontine tegmental nucleus. *Neuromodulation.* 2009;12(3):191-204.
24. Mazzone P, Scarnati E, Garcia-Rill E. Commentary: the pedunculopontine nucleus: clinical experience, basic questions and future directions. *J Neural Transm.* 2011;118(10):1391-1396.
25. Thevathasan W, Pogosyan A, Hyam JA, et al. Alpha oscillations in the pedunculopontine nucleus correlate with gait performance in parkinsonism. *Brain.* 2012;135(pt 1):148-160.
26. Mazzone P, Insola A, Lozano A, et al. Peripeduncular and pedunculopontine nuclei: a dispute on a clinically relevant target. *Neuroreport.* 2007;18(13):1407-1408.
27. Zrinzo L, Zrinzo LV, Hariz M. The pedunculopontine and peripeduncular nuclei: a tale of two structures. *Brain.* 2007;130(pt 6):e73.
28. Zrinzo L, Zrinzo LV. Surgical anatomy of the pedunculopontine and peripeduncular nuclei. *Br J Neurosurg.* 2008;22(suppl 1):S19-S24.
29. Zrinzo L, Zrinzo LV, Tisch S, et al. Stereotactic localization of the human pedunculopontine nucleus: atlas-based coordinates and validation of a magnetic resonance imaging protocol for direct localization. *Brain.* 2008;131(pt 6):1588-1598.
30. Mazzone P, Sposato S, Insola A, Scarnati E. The deep brain stimulation of the pedunculopontine tegmental nucleus: towards a new stereotactic neurosurgery. *J Neural Transm.* 2011;118(10):1431-1451.
31. Fahn S, Elton R. Members of the UPDRS Development Committee Unified Parkinson's disease rating scale. In: Fahn S, Marsden CD, Calne DB, Goldstein M, eds. *Recent Developments in Parkinson's Disease.* Floram Park, NY: Macmillan Healthcare Information; 1987:153-163.
32. Goetz CG, Poewe W, Rascol O, et al. Movement Disorder Society Task Force report on the Hoehn and Yahr staging scale: status and recommendations. *Mov Disord.* 2004;19(9):1020-1028.
33. Tsanas A, Little MA, McSharry PE, Scanlon BK, Papapetropoulos S. Statistical analysis and mapping of the Unified Parkinson's Disease Rating Scale to Hoehn and Yahr staging. *Parkinsonism Relat Disord.* 2012;18(5):697-699.
34. Schaltenbrand G, Wahren W. *Atlas for Stereotaxy of the Human Brain.* New York, NY: Thieme; 1977.
35. Paxinos G, Huang XF. *Atlas of the Human Brainstem.* San Diego, CA: Academic Press; 1995.
36. Rinne JO, Ma SY, Lee MS, Collan Y, Roytta M. Loss of cholinergic neurons in the pedunculopontine nucleus in Parkinson's disease is related to disability of the patients. *Parkinsonism Relat Disord.* 2008;14(7):553-557.
37. Zweig RM, Jankel WR, Hedreen JC, Mayeux R, Price DL. The pedunculopontine nucleus in Parkinson's disease. *Ann Neurol.* 1989;26(1):41-46.
38. Takakusaki K, Habaguchi T, Ohtinata-Sugimoto J, Saitoh K, Sakamoto T. Basal ganglia efferents to the brainstem centers controlling postural muscle tone and locomotion: a new concept for understanding motor disorders in basal ganglia dysfunction. *Neuroscience.* 2003;119:293-308.
39. Scarnati E, Florio T, Capozzo A, Confalone G, Mazzone P. The pedunculopontine tegmental nucleus: implications for a role in modulating spinal cord motoneuron excitability. *J Neural Transm.* 2011;118(10):1409-1421.
40. Karachi C, Andre A, Bertasi E, Bardin E, Lehericy S, Bernard FA. Functional parcellation of the lateral mesencephalus. *J Neurosci.* 2012;32(27):9396-9401.
41. Grabli D, Karachi C, Welter ML, et al. Normal and pathological gait: what we learn from Parkinson's disease. *J Neurol Neurosurg Psychiatry.* 2012;83(10):979-985.
42. Nowak LG, Bullier J. Axons, but not cell bodies, are activated by electrical stimulation in cortical gray matter. I. Evidence from chronaxie measurements. *Exp Brain Res.* 1998;118(4):477-488.
43. Moro E, Lozano AM, Pollak P, et al. Long-term results of a multicenter study on subthalamic and pallidal stimulation in Parkinson's disease. *Mov Disord.* 2010;25(5):578-586.
44. Odekerken VJ, van LT, Staal MJ, et al. Subthalamic nucleus versus globus pallidus bilateral deep brain stimulation for advanced Parkinson's disease (NSTAPS study): a randomised controlled trial. *Lancet Neurol.* 2013;12(1):37-44.
45. Caliendo P, Insola A, Scarnati E, et al. Effects of unilateral pedunculopontine stimulation on electromyographic activation patterns during gait in individual patients with Parkinson's disease. *J Neural Transm.* 2011;118:1477-1486.
46. Pierantozzi M, Palmieri MG, Galati S, et al. Pedunculopontine nucleus deep brain stimulation changes spinal cord excitability in Parkinson's disease patients. *J Neural Transm.* 2008;115(5):731-735.

## Acknowledgments

The authors wish to thank Dr M.G. Altibrandi and Dr F. Viselli, neurologists of the S. Giovanni Battista Hospital, Sovereign Military Order of Malta in Rome, for their clinical evaluations of patients.

## COMMENT

The authors provide an interesting analysis of the anatomy of the pedunculopontine tegmental nucleus (PPTg) as it relates to targeting deep brain stimulation (DBS) in this region to treat Parkinson disease (PD) and progressive supranuclear palsy (PSP) and responses to DBS. The topic is timely and relevant. PPTg has been proposed as a target for DBS to treat PD and PSP symptoms that do not respond to DBS of current standard targets (subthalamic nucleus and globus pallidus), but existing publications of PPTg DBS provide conflicting results regarding efficacy. A potential source of discrepancies between reported outcomes of PPTg

DBS is that PPTg is an ill-defined structure and there is a lack of clarity about which specific portion of the PPTg, if any, serves as the “ideal” target for DBS. The authors provide a detailed evaluation of brainstem anatomy with respect to PPTg, DBS lead locations, stimulation parameters, and clinical outcomes in a sizeable series of patients who underwent PPTg DBS. They conclude that variability of brainstem anatomy warrants individualized PPTg DBS targeting, but they report also a lack of correlation between lead position and outcomes, observing that benefits

of PPTg DBS may not be linked directly to the site of stimulation. This report provides further evidence in support of the utility of PPTg DBS for treatment of symptoms related to PD and PSP, but will likely stir further discussion about whether there is or is not a specific region within PPTg that is the preferred target for DBS.

**Kenneth A. Follett**  
*Omaha, Nebraska*

